

MMW Radar Scattering Statistics of Terrain At Near Grazing Incidence¹

R. D. De Roo, F. T. Ulaby, A. E. El-Rouby, and A. Y. Nashashibi

The Radiation Laboratory
Department of Electrical Engineering
and Computer Science
The University of Michigan
Ann Arbor, MI 48109-2122 USA

ABSTRACT

The statistical behavior of clutter observed near grazing incidence and at 95 GHz is investigated for the specific cases of bare ground, snow-cover, and for a heterogeneous scene. The bare ground constitutes a homogeneous target under homogeneous conditions and the magnitude of the amplitude is Rayleigh distributed. While the snow-cover is a homogeneous target, the conditions under which it was observed are heterogeneous, and the Bayes rule is employed to describe its clutter distribution. The Bayes rule integrates variations due to signal fading with the underlying variations in the backscattering coefficient associated with the heterogeneity. The heterogeneous scene is also successfully described with the Bayes rule.

¹This work was supported by Contract QK 8820 with Lockheed Sanders Inc., as part of the Army Research Laboratory's Federated Laboratory Advanced Sensors Project.

1 Introduction

The objective of this paper is to examine the nature of the statistical variability of radar clutter at millimeter wavelengths (MMW), with particular emphasis on observation directions corresponding to angles near grazing incidence. The statistical nature of terrain clutter variations have been explored at millimeter wavelengths (MMW) and angles far from grazing [1], and at grazing incidence but at lower frequencies [2], but the authors are not aware of any study of the statistics of MMW scattering of terrain near grazing incidence.

The Rayleigh distribution will be used to analyze MMW near-grazing clutter where the clutter is homogeneous, and where it is not, the Bayes rule will be employed to build up the observed distribution from subsets of the clutter which are homogeneous. An alternative would be to employ a more specific distribution such as the K -distribution, but while the K -distribution may adequately describe sea clutter [3, 4], the use of this distribution to describe terrain clutter has not met with unanimous success [5].

Open ground in early spring is used an example of a homogeneous target; snow-cover, under a variety of temperatures, is used as an example of a homogeneous target under different conditions; and an entire scene consisting of trees, bushes, and bare ground is used as an example of a heterogeneous target. First, we start with a brief description of the radar system used to acquire the data reported in this study.

2 95-GHz Measurement Program

From 4 March through 15 April 1994, the Army Research Laboratory (ARL) operated its 95 GHz polarimetric radar at a single site in Grayling, MI, as part of a study to characterize MMW scattering from terrain [6]. At preselected random dates and times, the radar performed a mission: it scanned the scene in Figure 1 in 1.0° steps in azimuth and at most 1.0° steps in elevation. The radar has a one-way beamwidth of 1.5° . To distinguish the measurements made in early 1994 from a set made in late 1993, these measurements are known collectively as Grayling II. In all, there were more than 170 missions at Grayling II.

The radar transmitted 100 ns pulses, giving the system a raw range resolution of 15 m. The polarization was switched between each pulse. For the purpose of sharpening the range resolution, subsequent pairs of pulses were transmitted with carrier frequencies 5 MHz apart. Each group of 256 pulses, with carrier frequencies ranging from 95.00 GHz to 95.64 GHz, is called a “ramp.” In this analysis, the frequency stepped data was used not for sharpening the range but to enlarge the



Figure 1: View from the radar of the Grayling II test site. The approximate locations of the pixels comprising bare ground at 5° depression are marked.

number of independent samples for each pixel, which is a single 15 m range bin at a given elevation and azimuth position of the radar. As the target decorrelation bandwidth [7] is 10 MHz, only every other frequency step was used, yielding $N_f = 64$ for the number of statistically decorrelated frequencies per ramp.

While the polarimetric measurements were made for both circular and linear polarizations, only the linear basis is used in this analysis. To reduce noise, the radar was allowed to dwell on each pixel for eight frequency ramps. Calibration, involving measurements of two trihedrals and three dihedrals, were performed before and after each mission and yielded a measurement accuracy of ± 1 dB [7]. Details of the experimental procedure, including polarimetric calibration, can be found in [6].

As can be seen in Figure 1, the scene is composed of trees and bushes interspersed in a relatively open space. In addition, a few hard targets were located in the scene for some missions for the purpose of testing Automatic Target Recognition algorithms. The composition of each pixel could be determined from a videotape recorded from a camera mounted on the gimbal with the radar. Very few pixels were visually homogeneous: most contained part of a tree or bush, or were partially obscured by such vegetation. At a depression angle of 5° , seven pixels were

identified from the videotape as comprising of only bare ground, the most at any one depression angle. These pixels ranged in azimuth from 63° to 70° (but excluding the pixel at 68° , which contained a single tall plant). For some missions, these pixels consisted of snow cover, while for other, later, missions the snow had melted away. Previous studies [8, 9] indicate that the extinction in snow is very high at millimeter wavelengths, and so the snow-cover can be considered a clutter type independent of the underlying ground. While it is not possible to positively identify the content of these pixels from the videotape, once the snow had melted it can be assumed they contained at most low dormant grasses. These pixels are used in the following tests for homogeneous targets; the entire scene was used for the heterogeneous target.

3 Homogeneous Terrain Under Homogeneous Conditions

A distributed target, such as a terrain surface, is said to be homogeneous with regard to a particular property if that property is spatially invariant over the extent of the target; i.e., it assumes the same value everywhere. From a radar standpoint, a homogeneous distributed target is one that exhibits a constant backscattering cross section per unit area for all pixels when illuminated by a very wide bandwidth incoherent signal, akin to solar illumination in the visible part of the spectrum. In practice, however, radar uses a coherent signal with a relatively narrow bandwidth and that bandwidth is usually used to attain good range resolution. Consequently, a radar image of such a distributed target would exhibit a “salt and pepper” appearance, usually referred to as image speckle. A computer generated speckled image of a homogeneous distributed target is shown in Fig. 2. Speckle is a result of coherent signal interference associated with the vector addition of phasors corresponding to the backscatter from all of the scattering centers within a given pixel. If at the resolution scale:

- (1) each resolution cell of area A contains a large number of scatterers, so that the central limit theorem is applicable,
- (2) all the scatterers produce backscatter responses of comparable magnitude,
- (3) the scatterers are randomly distributed in location within the resolution cell,
- (4) the range extent of the target illuminated by the radar is smaller than the mean range to the target, and
- (5) the range extent of the target is many wavelengths across,

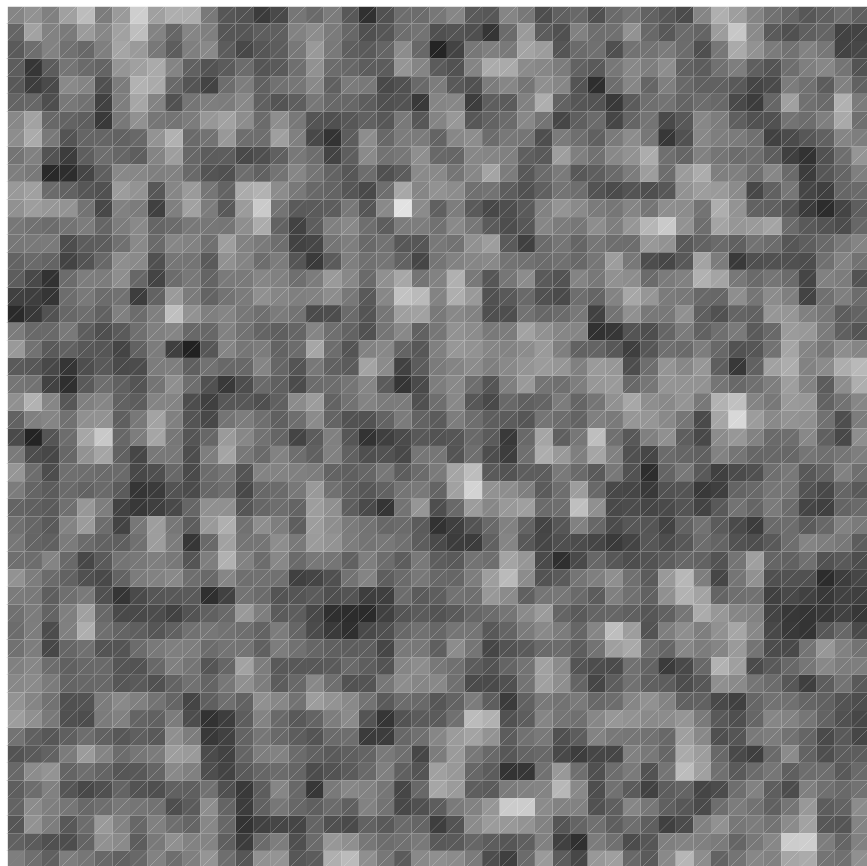


Figure 2: Computer simulation of a speckled radar image after linear detection.

then the target is a statistically homogeneous target and the scattering process is governed by Rayleigh fading statistics [1, 10].

Assumptions (1) through (5) are almost always satisfied in practice, but not always. A high-resolution radar with resolution cell dimensions on the order of centimeters or decimeters may not contain enough independent scatterers to satisfy assumption (1). The consequences of such a situation have been examined by Daba and Bell [11]. Another assumption that is sometimes violated is assumption (2), requiring that no single scatterer (or very few scatterers) dominates all others. The statistics for scattering by a single large scatterer embedded in a background of many smaller randomly distributed scatterers are characterized by the Rice distribution [12].

pdf of Scattering Amplitudes

Assume a polarimetric radar image of homogeneous terrain consists of a large number of pixels, N , each of area A . For each pixel, the backscatter measured by the system is in the form of the scattering matrix \mathbf{S} , where [13]:

$$\mathbf{S} = \begin{bmatrix} S_{vv} & S_{vh} \\ S_{hv} & S_{hh} \end{bmatrix}. \quad (1)$$

The elements of \mathbf{S} are the complex scattering amplitudes associated with the four different combinations of transmit and receive linear polarizations. Element S , where S represents any one of S_{vv} , S_{vh} , S_{hv} or S_{hh} , may be expressed as

$$S = S' + j S'' = |S|e^{j\phi}, \quad (2)$$

where $S' = \text{Re}[S]$, $S'' = \text{Im}[S]$, $|S|$ is the magnitude of S and ϕ is its phase angle. The joint probability density function of the real and imaginary parts of S are each Gaussian distributed with zero means and equal variances and is given by

$$p(S', S'') = \frac{1}{2\pi s^2} \exp \left[- \left(S'^2 + S''^2 \right) / 2 s^2 \right] \quad (3)$$

where s is the standard deviation.

Figure 3 compares the measured histograms of S'_{vv} and S''_{vv} with zero-mean Gaussian pdfs with variances equal to those obtained from the histograms. The measurements, which were made for the bare ground pixels at a depression angle of 5° , were part of the last segment of the Grayling II expedition, during which time the snow cover had already melted away. For missions 150, 155-157, and 163-170 the ground was bare, temperatures were above freezing and there was no precipitation. Over all these missions, the VV-polarized normalized (with respect

to pixel area A) radar cross section (RCS), calculated for each pixel by averaging over the 64 frequency samples and 8 ramps for each pixel, had a mean of -22.83 dB and a standard deviation of 0.70 dB. For perfect calibration, an RCS measurement based on 64 independent samples has an associated uncertainty of 0.51 dB. Hence it is safe to assume that these samples represent a homogeneous target under homogeneous conditions.

As can be seen from the data shown in Fig. 3 the measured means of S'_{vv} and S''_{vv} are both approximately zero, their standard deviations s'_{vv} and s''_{vv} are approximately equal, and the histograms are well represented by the Gaussian pdf.

Also, the calculated correlation coefficient between S'_{vv} and S''_{vv} was found to be 0.0158, which means that they are essentially uncorrelated.

Similar results were observed for the other polarization components of the matrix \mathbf{S} .

pdf for Received Voltage Magnitude

If S' and S'' are each zero-mean Gaussian random variables with equal variances ($s' = s'' = s$) and if, additionally, S' and S'' are uncorrelated, then the pdf of $|S|$ is Rayleigh distributed [1, 10, 14]. The pdf of $V = 2\sqrt{\pi}|S|$ is given by

$$p(V \mid \bar{V}) = \frac{\pi}{2} \frac{V}{\bar{V}^2} \exp\left[-\frac{\pi}{4}(V/\bar{V})^2\right], \quad V \geq 0, \quad (4)$$

where \bar{V} is the mean value of V and it is related to the standard deviation s by

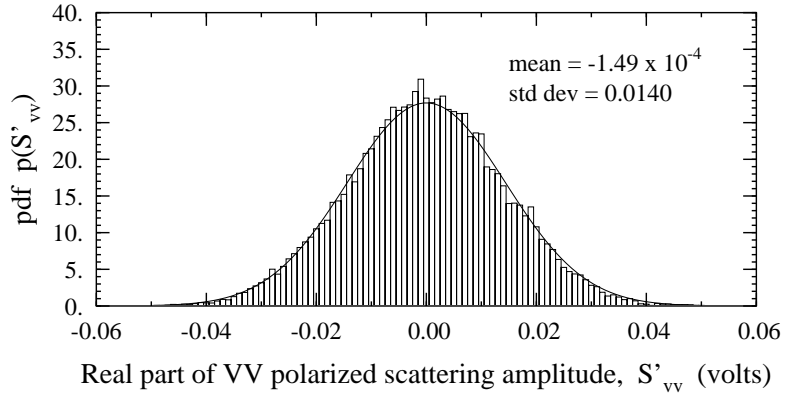
$$\bar{V} = \sqrt{\frac{\pi}{2}}(2\sqrt{\pi}s) = \sqrt{2}\pi s \quad (5)$$

Measured and calculated pdfs are compared in Fig. 4(a) for VV and cross polarizations. The Rayleigh model appears to provide excellent fits to the data of the bare ground pixels, confirming that they constitute a homogeneous target under homogeneous conditions.

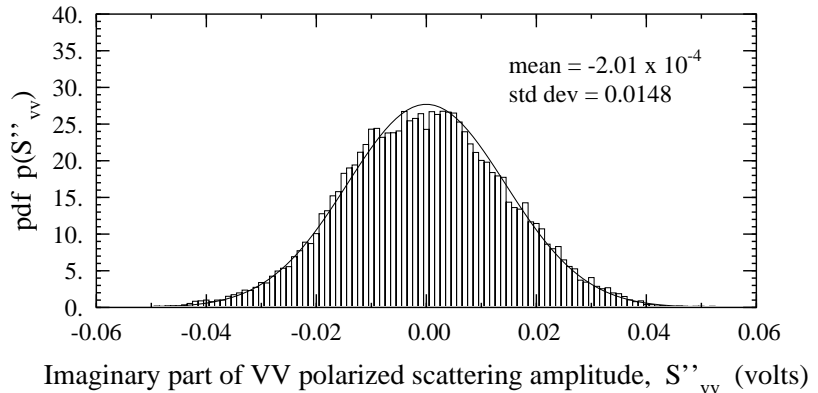
The term “Rayleigh fading” is used to describe the scattering process for any quantity associated with statistically homogeneous clutter, even though it is only the received voltage magnitude which is Rayleigh distributed.

pdf for Intensity

For intensity (power) or intensity related quantities, such as the radar cross section per unit area when expressed in units of (m^2/m^2) , the pdf for a single

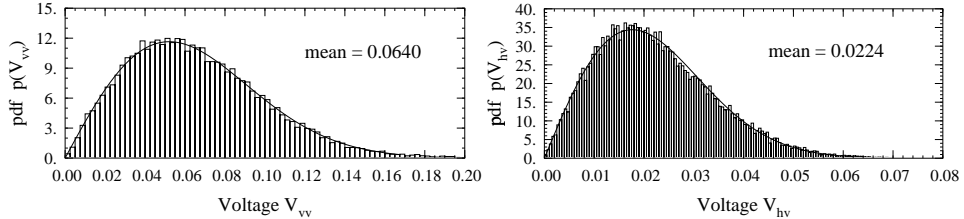


(a)

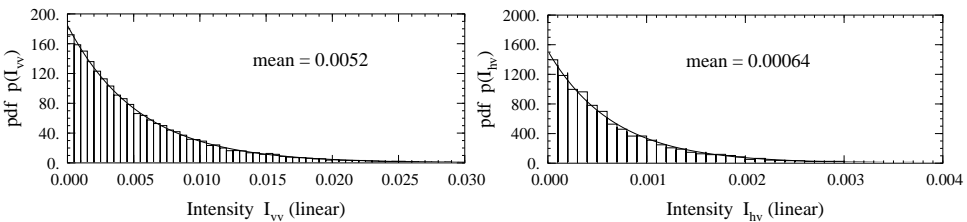


(b)

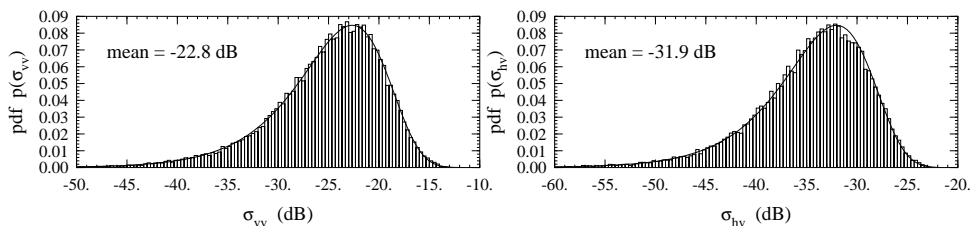
Figure 3: Histograms of the VV-polarized scattering amplitude and corresponding Gaussian distributions with the same variance, for Grayling II pixels of bare ground, a homogeneous target under homogeneous conditions. The sample set is composed of 64 frequency samples \times 8 ramps \times 7 pixels \times 12 missions = 43008 data points.



(a) Linear detection histogram and the Rayleigh distribution.



(b) Square law detection histogram and the exponential distribution, for linear power.



(c) Square law detection histogram and the exponential distribution displayed logarithmically on a decibel scale.

Figure 4: Histograms of the Grayling II pixels of bare ground, a homogeneous target under homogeneous conditions, for linear detection and square law detection. The same sample set is used as in the previous figure. The left column is for VV polarization; the right column is for HV polarization.

sample drawn from a population with mean $\bar{I} = \frac{4}{\pi} \bar{V}^2$ becomes an exponential [10, 14]:

$$p(I | \bar{I}) = \frac{1}{\bar{I}} \exp[-I/\bar{I}], \quad I \geq 0 \quad (6)$$

where \bar{I} is the mean value of $I = V^2 = 4\pi|S|^2$. Figure 4(b) compares the measured pdfs for I_{vv} and I_{hv} with the exponential pdf based on (6). Excellent agreement is observed in both cases.

pdf for Normalized RCS in dB

Through a transformation of variables from I to $\sigma = 10 \log I$ we obtain the pdf

$$p(\sigma | \bar{\sigma}) = \frac{\ln 10}{10} z e^{-z}, \quad (7)$$

with

$$z = 10^{(\sigma - \bar{\sigma})/10}, \quad (8)$$

and $\bar{\sigma} = 10 \log \bar{I}$. We note that $\bar{\sigma}$, which is commonly called the *backscattering coefficient* and denoted by the symbol σ^0 , is determined by calculating \bar{I} first and then converting it into dB, and not by evaluating the average value of σ . That is, $\bar{\sigma} \neq \langle 10 \log I \rangle$. For the case where all values of I are first converted to dB and then they are used to determine the mean value, the reader is referred to Hoekman [15].

Figure 4(c), which includes calculated and measured pdfs for σ , is a further confirmation that the Rayleigh model is appropriate for characterizing MMW near-grazing backscatter statistics for homogeneous terrain under homogeneous conditions.

4 Homogeneous Terrain Under Heterogeneous Conditions

We will now examine the same pixels that were discussed in the preceding section, but under a variety of different snow-cover conditions. During missions 9-13, the snow was wet; during missions 18-24, the snow was refrozen; and during missions 93, 94, and 131-134, the snow was fresh. Figure 5 displays the histograms of the

mean value of the normalized RCS for VV and cross polarizations, $p(\bar{\sigma}_{vv})$ and $p(\bar{\sigma}_{hv})$, constructed from data for 8 ramps at 7 pixels over 18 missions. For each pixel, $\bar{\sigma}_{vv}$ and $\bar{\sigma}_{hv}$ are determined by averaging over the 64 independent frequency samples, which means that the precision associated with each measurement of $\bar{\sigma}$ is about ± 0.5 dB. Each histogram exhibits a dynamic range on the order of 20 dB, all essentially due to the varying snow-cover conditions. If a scene with such a backscatter histogram were to be imaged by a one-look per pixel radar, the observed intensity of the resultant speckled radar image would be characterized by a pdf given by the Bayes rule as [16]:

$$p(I) = \int_0^\infty p(I | \bar{I}) p(\bar{I}) d\bar{I} \quad (9)$$

where \bar{I} is the mean intensity (corresponding to $\bar{\sigma}$ in dB) and $p(\bar{I})$ is the pdf corresponding to the histograms shown in Fig. 5. To evaluate the applicability of the Bayes formula to the available data, we should first convert (9) into a summation over the number of observations $N_0 = 7 \text{ pixels} \times 8 \text{ ramps} \times 18 \text{ missions} = 1008$. If we denote by \bar{I}_k the mean value obtained by averaging the 64 independent frequency measurements for a given ramp/pixel/and mission combination, then (9) may be rewritten as

$$p(I) = \frac{1}{N_0} \sum_{k=1}^{N_0} \frac{1}{\bar{I}_k} \exp(-I/\bar{I}_k) \quad (10)$$

where we have replaced $p(I | \bar{I})$ with the exponential pdf given by (6).

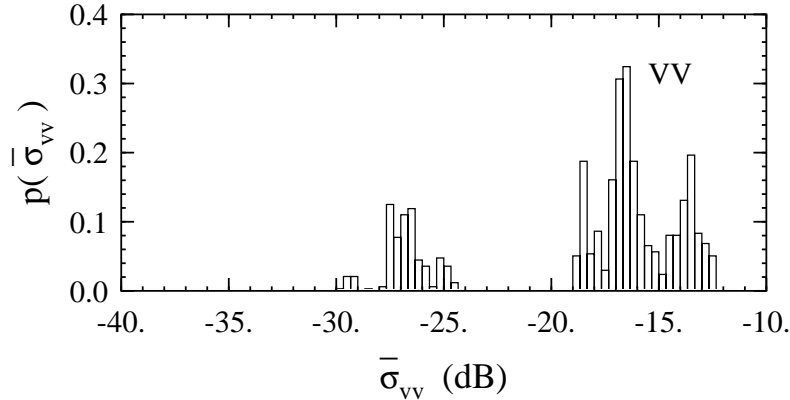
For linear detection, the equivalent expressions are

$$p(V) = \int_0^\infty p(V | \bar{V}) p(\bar{V}) d\bar{V} \quad (11)$$

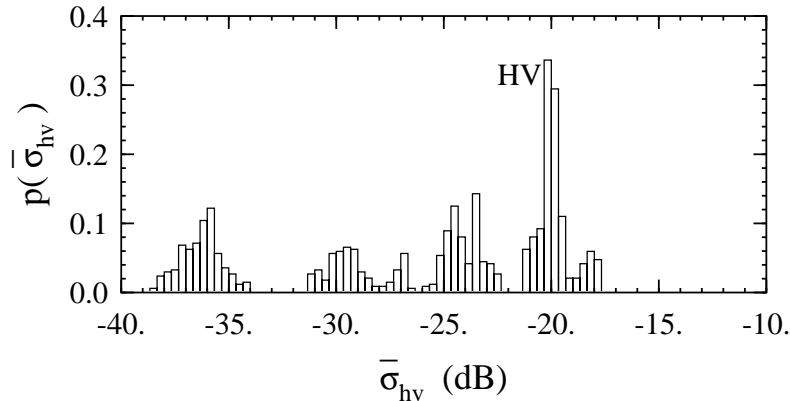
for the continuous case, and

$$p(V) = \frac{\pi}{2N_0} \sum_{k=1}^{N_0} \frac{V}{V_k^2} \exp\left[-\frac{\pi}{4}\left(\frac{V}{V_k}\right)^2\right] \quad (12)$$

for the discrete case. Figure 6 compares histograms based on the observed voltage or intensity, with pdfs calculated on the basis of (10) and (12) using the pixel mean distributions shown in Fig. 5. Excellent agreement is observed in all cases.

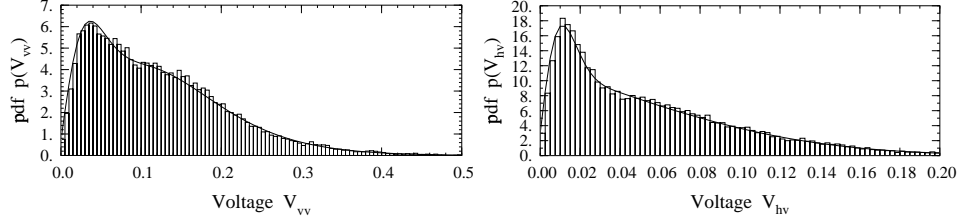


(a)

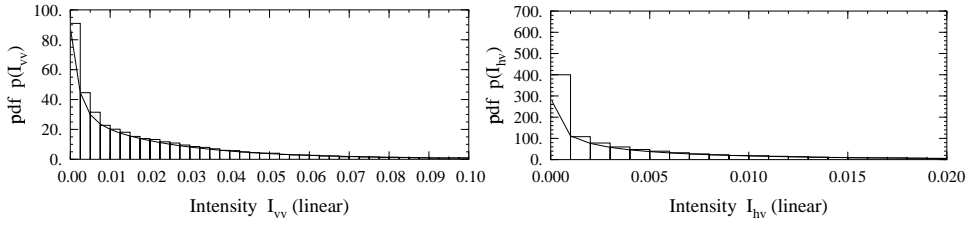


(b)

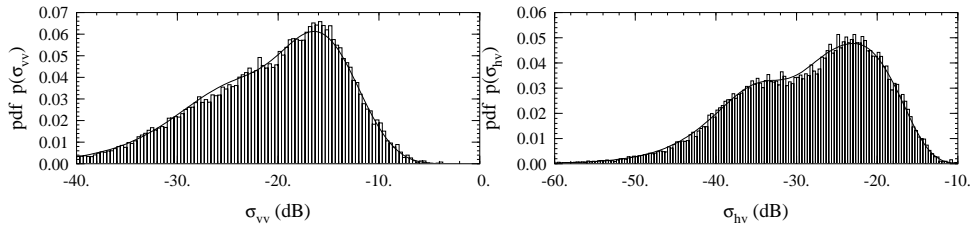
Figure 5: Histograms of the mean values of the Grayling II pixels of snow over bare ground, a homogeneous target under heterogeneous conditions. The sample set is composed of 64 frequency samples \times 8 ramps \times 7 pixels \times 18 missions = 64512 data points; frequency averaging was used to obtain the distribution of the backscattering coefficients, so each histogram represents 1008 σ^0 values. The variations due to different missions are greater than those due to different pixels and ramps, giving rise to some clumping of the data. Part (a) is for VV-polarization and part (b) is for HV polarization. For comparison, the mean values of the bare ground itself, a homogeneous target under homogeneous conditions, has a standard deviation of only 0.70 dB.



(a) Linear detection histogram and the Rayleigh distribution.



(b) Square law detection histogram and the exponential distribution, for linear power.



(c) Square law detection histogram and the exponential distribution displayed logarithmically on a decibel scale.

Figure 6: Histograms of the Grayling II pixels of snow over bare ground, showing the results of the application of the Bayes formula. The same sample set is used as in the previous figure.

5 Heterogeneous Terrain

Because heterogeneous terrain exhibits a wide range of backscattering values, some authors have resorted to the use of non-physically based multi-parameter distributions, such as the K -distribution, to characterize the observed pdf of radar clutter [3, 5, 17]. The K -distribution, while popular, is ultimately based on an assumption of a Gamma distribution for the mean pixel RCS [16] which Jao [18], despite various rigorous derivations and several plausibility arguments, admits is “purely hypothetical.” We prefer instead to apply the more general Bayes formula introduced in the preceding section, and to demonstrate its applicability we have used the data acquired from an entire scene, which includes a variety of different terrain classes as can be seen from the photograph of Fig. 1.

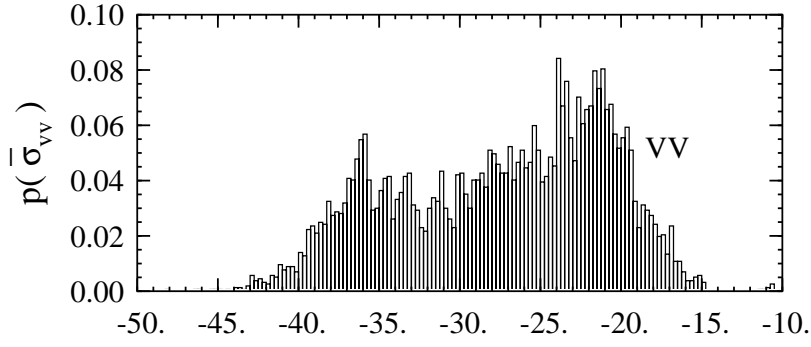
The distribution of the normalized mean pixel RCS, $p(\bar{\sigma})$, is shown in Fig. 7 and the clutter pdfs are shown in Fig. 8. The data are non-Rayleigh, because the clutter histograms in Fig. 8 are clearly not the same shape as those in Fig. 4. Also, the distributions of the mean pixel RCS in Fig. 7 are clearly not the smooth bell-shaped curve of the Gamma distribution, implying that the K -distribution is inappropriate in this circumstance.

Despite the fact that in the scene very few pixels together comprise a homogeneous target, the fit of the calculated distributions, using (10) and (12), to the measured distributions is excellent. This is because for each pixel, the different frequency samples in each ramp constitute an independent observation of the same target, enforcing the homogeneity required to make an estimate of the RCS under Rayleigh conditions [7]. That is, while assumption 2 of Section 3 is violated in this heterogeneous scene when comparing one pixel to the next, within each pixel it is satisfied when comparing different frequency samples. Thus, the characterization of the distribution of terrain clutter is a task of characterizing the distribution of the σ^0 of homogeneous pieces of terrain. Where spatially homogeneous regions of terrain, such as bare ground or snow-cover under uniform conditions, do not exist, it is possible to achieve such homogeneity via frequency averaging.

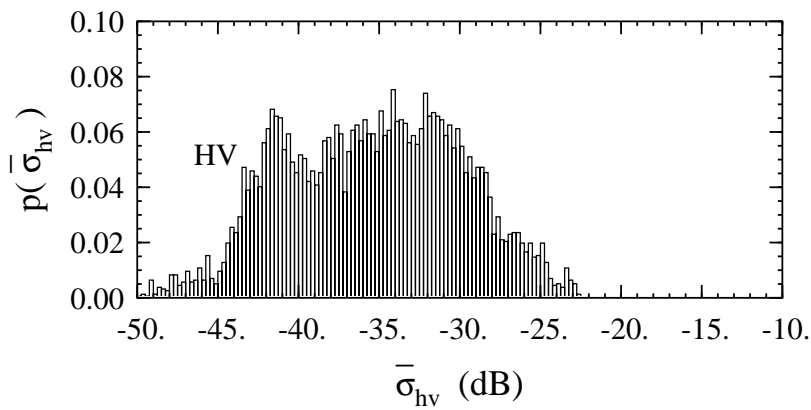
6 Concluding Remarks

The fading statistics of radar backscatter were investigated using 95-GHz near-grazing measurements of terrain. This study:

- (a) confirmed that the Rayleigh fading model is quite suitable for characterizing the backscatter distribution for homogeneous terrain under homogeneous conditions, as exemplified by bare ground, and
- (b) demonstrated that the Bayes formula provides a physically based approach for

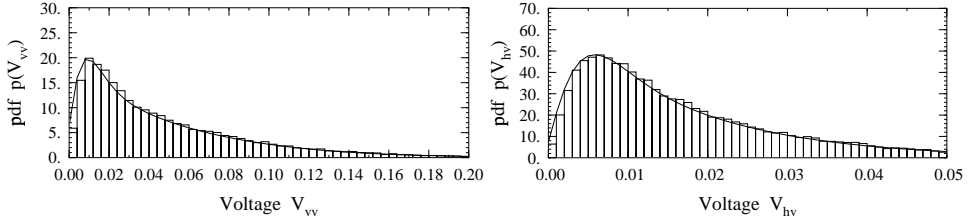


(a)

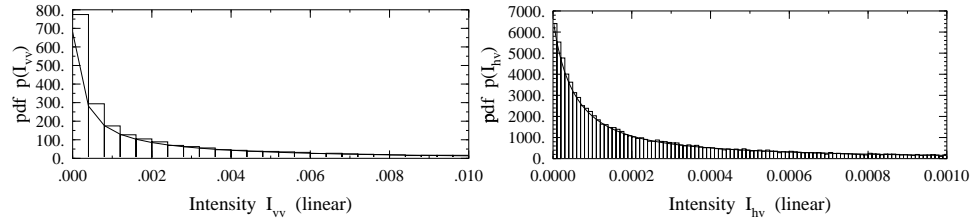


(b)

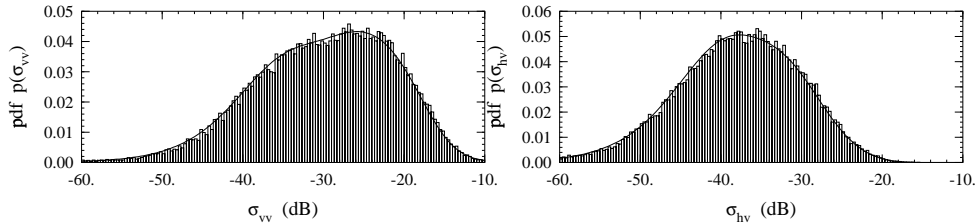
Figure 7: Histograms of mean values of the Grayling II pixels of the entire scene of mission 155, a heterogeneous target. The sample set is composed of 64 frequency samples \times 1 ramp \times 784 pixels over 1 mission = 50176 data points; frequency averaging was used to obtain the distribution of the backscattering coefficients, so each histogram represents 784 σ^0 values. Part (a) is for VV-polarization and part (b) is for HV polarization.



(a) Linear detection histogram and the Rayleigh distribution.



(b) Square law detection histogram and the exponential distribution, for linear power.



(c) Square law detection histogram and the exponential distribution displayed logarithmically on a decibel scale.

Figure 8: Histograms of the Grayling II pixels of the entire scene of mission 155, showing the results of the application of the Bayes formula. The same sample set is used as in the previous figure.

characterizing the distributions for both snow-cover at different states of freshness and wetness, as an example of homogeneous terrain under heterogeneous conditions, and for an entire scene consisting of mixed open space and several types of trees, as an example of heterogeneous terrain.

The use of frequency averaging on individual pixels of an image allows for the generation of mean RCS values over homogeneous subregions of the image, since each pixel is homogeneous between frequency points. Thus, the Bayes formula is capable of describing the distribution of clutter of even heterogeneous scenes, provided the mean RCS values of the objects constituting the scene can be described. In this paper, we allowed the data itself to provide the distribution of mean RCS values, because it does not conform to any simple closed-form probability density function.

Acknowledgments

The authors wish to express their sincere thanks and appreciation to Mr. Ron Wellman and his colleagues of the Army Research Laboratory, Adelphi, MD, for making their MMW backscatter data available to the University of Michigan.

References

- [1] F. T. Ulaby, T. F. Haddock, and R. T. Austin, “Fluctuation statistics of millimeter-wave scattering from distributed targets,” *IEEE Transactions on Geoscience and Remote Sensing*, vol. 26, no. 3, pp. 268–281, May 1988.
- [2] J. B. Billingsley, “Ground clutter measurements for surface-sited radar,” Technical Report 786 rev. 1, Lincoln Laboratory, Lexington, MA, February 1 1993.
- [3] E. Jakeman and P. N. Pusey, “A model for non-Rayleigh sea echo,” *IEEE Transactions on Antennas and Propagation*, vol. 24, no. 6, pp. 806–814, November 1976.
- [4] K. D. Ward and S. Watts, “Radar sea clutter,” *Microwave Journal*, pp. 109–120, June 1985.
- [5] A. C. Frery, H.-J. Müller, C. da Costa Freitas Yanassee, and S. J. S. Sant’Anna, “A model for extremely heterogeneous clutter,” *IEEE Transactions on Geoscience and Remote Sensing*, vol. 35, no. 3, pp. 648–659, May 1997.

- [6] R. Wellman, G. Goldman, J. Silvious, and D. Hutchins, “Analyses of millimeter wave radar low-angle ground-clutter measurements for European-like and desert environments,” Technical Report ARL-TR-1102, US Army Research Laboratory, Adelphi, MD, July 1996.
- [7] F. T. Ulaby, A. Nashashibi, A. El-Rouby, E. S. Li, R. D. De Roo, K. Sarabandi, R. J. Wellman, and H. B. Wallace, “95-GHz scattering by terrain at near-grazing incidence,” *IEEE Transactions on Antennas and Propagation*, vol. 46, no. 1, pp. 3–13, January 1998.
- [8] Y. Kuga, F. T. Ulaby, T. F. Haddock, and R. D. De Roo, “Millimeter-wave radar scattering from snow: 1. radiative transfer model,” *Radio Science*, vol. 26, no. 2, pp. 329–341, March–April 1991.
- [9] P. S. Chang, J. B. Mead, E. J. Knapp, G. A. Sadowy, R. E. Davis, and R. E. McIntosh, “Polarimetric backscatter from fresh and metamorphic snowcover at millimeter wavelengths,” *IEEE Transactions on Antennas and Propagation*, vol. 44, no. 1, pp. 58–73, January 1996.
- [10] F. T. Ulaby and M. C. Dobson, *Handbook of Radar Scattering Statistics for Terrain*, Artech House, Norwood, MA, 1989.
- [11] J. S. Daba and M. R. Bell, “Statistics of the scattering cross-section of a small number of random scatterers,” *IEEE Transactions on Antennas and Propagation*, vol. 43, no. 8, pp. 773–783, August 1995.
- [12] S. O. Rice, “Mathematical analysis of random noise, Parts III & IV,” *Bell System Technical Journal*, vol. 24, pp. 46–156, July 1945.
- [13] F. T. Ulaby and E. C. Elachi, *Radar Polarimetry for Geoscience Applications*, Artech House, Norwood, MA, 1990.
- [14] F. T. Ulaby, R. K. Moore, and A. K. Fung, *Microwave Remote Sensing: Active and Passive*, volume 2, Addison-Wesley, Reading, MA, 1982.
- [15] D. H. Hoekman, “Speckle ensemble statistics of logarithmically scaled data,” *IEEE Transactions on Geoscience and Remote Sensing*, vol. 29, no. 1, pp. 180–182, January 1991.
- [16] D. J. Lewinski, “Nonstationary probabilistic target and clutter scattering models,” *IEEE Transactions on Antennas and Propagation*, vol. 31, no. 3, pp. 490–498, May 1983.

- [17] S. H. Yueh, J. A. Kong, J. K. Jao, R. T. Shin, and L. M. Novak, “K-distribution and polarimetric terrain radar clutter,” *Journal of Electromagnetic Waves and Applications*, vol. 3, no. 8, pp. 747–768, 1989.
- [18] J. K. Jao, “Amplitude distribution of composite terrain radar clutter and the K-distribution,” *IEEE Transactions on Antennas and Propagation*, vol. 32, no. 10, pp. 1049–1062, October 1984.